

Oscillation effects on neutrino decoupling in the early universe

Steen Hannestad

NORDITA, Blegdamsvej 17, DK-2100 Copenhagen, Denmark

(February 7, 2020)

In the early universe, neutrinos decouple from equilibrium with the electromagnetic plasma at a temperature which is only slightly higher than the temperature where electrons and positrons annihilate. Therefore neutrinos to some extent share in the entropy transfer from e^+e^- to other species, and their final temperature is slightly higher than the canonical value $T_\nu = (4/11)^{1/3}T_\gamma$. We study neutrino decoupling in the early universe with effects of neutrino oscillations included, and find that the change in neutrino energy density from e^+e^- annihilations can be about 2-3% higher if oscillation are included. The primordial helium abundance can be changed by as much as 1.5×10^{-4} by neutrino oscillations.

PACS numbers: 95.30.Cq,14.60.Pq,14.60.Lm,13.15.+g

I. INTRODUCTION

Freeze-out of particle species from thermal equilibrium is one of the most important features of the early universe. One example is supersymmetric cold dark matter such as the neutralino. If these particles were kept in thermal equilibrium throughout the history of the universe their present day abundance would be suppressed by a huge factor because of their large mass. However, because of their weak interactions, the pair annihilation processes which keep the particles in equilibrium stop being efficient as a temperature of the order $T \sim m/20$ [1]. At this time the particles decouple from equilibrium and their abundance is afterwards only diluted by cosmological expansion. Therefore such particles can be sufficiently abundant today to make up the dark matter [1].

In the present paper we discuss the decoupling of neutrinos from thermal equilibrium at a temperature of ~ 1 MeV. In the canonical picture the electron neutrinos decouple at a temperature of about 2 MeV, whereas the μ and τ neutrinos, which do not have charged current interactions, decouple at roughly 4 MeV. Shortly after this decoupling the temperature drops below the rest mass of the electron and electrons and positrons pair annihilate and dump their entropy into photons. The neutrinos are not supposed to share in this entropy transfer and therefore their temperature is lower than the photon temperature by a factor $(4/11)^{1/3}$ [2]. It is also implicit in this treatment that oscillations between active neutrino species have no effect because their distributions remain identical.

However, because the temperature difference between neutrino decoupling and electron-positron annihilation (at $T \sim m_e/3$) is only one order of magnitude the neutrinos will to some extent share in the entropy transfer and the final temperature of the neutrinos will be slightly different from the canonical value.

This problem has been treated many times in the past with various methods [3–14]. Early calculations made various approximations [3–5], whereas recent treatments have included solving the full momentum dependent system of Boltzmann equations including all neutrino reactions [6–13].

In all treatments so far, however, neutrinos have been assumed to be non-mixed species (although the possibility that neutrino heating could be changed by oscillations was mentioned in Ref. [15]). The recent results from the Sudbury Neutrino Observatory (SNO) [16] experiment have confirmed that the Solar neutrino deficit is indeed explained by active-active neutrino oscillations, most likely $\nu_e - \nu_\mu$ oscillations. However, the specific values of the mixing parameters have not been conclusively measured. At present there are four different solution regions in mixing parameter space. The best fit points for these four solutions (from Ref. [17]) are listed in Table I.

TABLE I. Best fit values of mixing parameters for solar neutrino solutions, as well as their goodness of fit.

Solution	$\delta m^2/eV^2$	$\sin 2\theta_0$	goodness of fit
Large Mixing Angle (LMA)	4.5×10^{-5}	0.91	59%
Small Mixing Angle (SMA)	4.5×10^{-5}	3.94×10^{-2}	19%
Low	1.0×10^{-7}	0.99	45%
Vacuum (VAC)	4.6×10^{-10}	0.91	42%

Also, by far the best explanation for the atmospheric neutrino problem is oscillations with maximal mixing between ν_μ and another neutrino, most likely ν_τ , as suggested by the Super-Kamiokande experiment [18]. In the present paper we treat neutrino decoupling in the early universe, taking into account neutrino oscillations. Unfortunately the numerical complexity of the problem increases dramatically if oscillations are introduced. We therefore treat the problem in the so-called quantum rate equation approximation where the momentum dependence of the problem is integrated out. We also refrain from treating the full three-flavour oscillation problem and concentrate on $\nu_e - \nu_\mu$ oscillations while assuming that ν_τ is unmixed. Data on atmospheric neutrinos suggest that ν_μ and ν_τ are in fact maximally mixed, and our assumption is therefore not likely to hold. We will discuss this issue more thoroughly in Section IV.

We find that neutrino heating is slightly more efficient if oscillations are included. For non-oscillating neutrinos we find an increase in neutrino energy density of $\Delta N_\nu \simeq 0.0467$, where $\Delta N_\nu = \delta\rho/\rho_*$ and $\rho_* = \frac{7}{8} \left(\frac{4}{11}\right)^{4/3} \rho_\gamma$. In the case of very efficient mixing of ν_e and ν_μ this is changed to $\Delta N_\nu \simeq 0.0479$, a change of 2.5%. We also find that oscillations can change the primordial helium abundance. Neutrino heating induces a change of $\Delta Y_P \simeq 1.2 \times 10^{-4}$ for non-oscillating neutrinos. For maximal mixing this is changed to $\Delta Y_P \simeq 2.2 \times 10^{-4}$, i.e. a difference comparable to the total magnitude of the effect. In the limiting case of complete mixing of all neutrinos the result is $\Delta N_\nu \simeq 0.0486$ and $\Delta Y_P \simeq 2.5 \times 10^{-4}$.

The next section contains a discussion of the essential rate equations needed to treat neutrino decoupling, as well as the equations needed to treat the cosmological expansion. Section III concerns the numerical details and results from solving the equations, and Section IV contains a discussion and conclusion. Finally, the Appendix contains various mathematical detail.

II. BOLTZMANN EQUATIONS

The fundamental equation describing the evolution of all particle species in the early universe is the Boltzmann equation, which for a non-mixed species is [19]

$$\frac{df}{dt} = \sum_i C_i[f], \quad (1)$$

where $C_i[f]$ are the collision terms. In a homogeneous and isotropic system $df/dt = \partial f/\partial t$. For the moment we do not consider the expansion of the universe, but this will be discussed at the end of the section.

However, for a treatment of oscillating neutrinos it is necessary to replace the single particle distribution function with the density matrix, ρ , for the mixed species. For neutrinos the density matrix is a 3×3 matrix, but in the present work we limit ourselves to studying two-flavor oscillations, with the third neutrino being non-mixed (in practice we study $\nu_e - \nu_\mu$ oscillations with ν_τ being non-mixed). The density matrix for neutrinos can then be written as

$$\rho(p) = \frac{1}{2}[P_0(p) + \mathbf{P}(p) \cdot \boldsymbol{\sigma}], \quad (2)$$

where σ_i are the Pauli matrices. An equivalent expression holds for anti-neutrinos. Notice that this definition is slightly different from the notation which is most often used $\rho(p) = \frac{1}{2}P_0(p)[1 + \mathbf{P}(p) \cdot \boldsymbol{\sigma}]$. This notation has the advantage that \mathbf{P} describes the internal state of the mixed neutrinos, whereas in our notation it does not. On the other hand our notation significantly simplifies the equations because it is linear (i.e. it does not contain a $P_0\mathbf{P}$ term). The convention we use is the same as that used by McKellar and Thomson [20] in their treatment of active-active oscillations in the early universe. The material in this section follows their treatment closely in several respects.

The usual one-particle distribution functions are the diagonal elements of the density matrix so that, $n_\alpha(p) = \frac{1}{2}[P_0(p) + P_z(p)]$ and $n_\beta(p) = \frac{1}{2}[P_0(p) - P_z(p)]$.

The mixed neutrinos, described by (P_0, \mathbf{P}) then evolve according to the equations

$$\dot{\mathbf{P}}(p) = \mathbf{V} \times \mathbf{P} + [R_\alpha(p) - R_\beta(k)]\hat{\mathbf{z}} - D(p)P_T(p) \quad (3)$$

$$+ \int dp' d(p, p') \mathbf{P}_T(p') - \mathbf{C}(p)P_0(p) + \int dp' \mathbf{c}(p, p') P_0(p') \quad (4)$$

$$\dot{P}_0(p) = R_\alpha(p) + R_\beta(p), \quad (5)$$

where $\mathbf{P}_T = P_x(p)\hat{\mathbf{x}} + P_y(p)\hat{\mathbf{y}}$ is the transversal component of the polarization vector \mathbf{P} . The rate terms are given by

$$R_i(p) = \int dp' dk dk' \left[\sum_j F_{ij}(pk|p'k') [n_j(k')n_j(p') - n_i(k)n_i(p)] \right. \quad (6)$$

$$\left. - \frac{1}{2} \sum_l G_l(k'p'|kp) \mathbf{P}_T(p) \cdot \bar{\mathbf{P}}_T^*(k) \right], \quad (7)$$

where \sum_j is over all weakly interacting species and \sum_l is over all other particles than the mixed neutrinos. In all cases $\int dq$ is taken to mean integration over phase space in the sense $\int dq = \int \frac{d^3\mathbf{q}}{(2\pi)^3}$.

Here, the first term in the brackets is the usual Boltzmann equation with exactly the same structure as for a non-mixed species. The second term arises due to the possibility that mixed state neutrinos annihilate with mixed state anti-neutrinos. This term therefore is only present for active-active oscillations where both states are interacting. The matrix element terms F and G are given by

$$F_{ij}(pk|p'k') = 2\pi NV^2(j(p), \bar{j}(k)|i(p'), \bar{i}(k'))\delta(p+k-p'-k') \quad (8)$$

$$G_l(pk|p'k') = 2\pi NV(\nu_\alpha(p'), \bar{\nu}_\alpha(k')|l(k), \bar{l}(p)) \quad (9)$$

$$\times V(\nu_\beta(p'), \bar{\nu}_\beta(k')|l(k), \bar{l}(p))\delta(p+k-p'-k'). \quad (10)$$

All the non-mixed species evolve according to the standard Boltzmann equation

$$\dot{n}_i(p) = \int dp' dk dk' \left[\sum_j F_{ij}(pk|p'k') [n_j(k')n_j(p') - n_i(k)n_i(p)] \right. \quad (11)$$

$$\left. + G_i(kp|k'p') \mathbf{P}_T(p) \cdot \bar{\mathbf{P}}_T^*(k) \right], \quad (12)$$

where again \sum_j goes over all species. As before there is a new term which arises from annihilation of mixed states. The terms in Eq. (4) containing \mathbf{c} , \mathbf{C} , D and d are damping terms from elastic and inelastic scatterings which break coherence of the oscillations. Details of how to calculate these terms can be found in Ref. [20].

Finally, the $\mathbf{V} \times \mathbf{P}$ term is the usual oscillation term which is responsible for the flavour oscillations. The potential vector \mathbf{V} can be written as

$$\mathbf{V} = 2E_{\alpha\beta}\hat{\mathbf{x}} + (E_{\alpha\alpha} - E_{\beta\beta})\hat{\mathbf{z}}. \quad (13)$$

Here,

$$E_{\alpha\beta} = \frac{\delta m^2}{2p} \sin 2\theta_0 - V_{\alpha\beta}(p) \quad (14)$$

$$E_{\alpha\alpha} - E_{\beta\beta} = -\frac{\delta m^2}{2p} \cos 2\theta_0 + V_\alpha(p) - V_\beta(p), \quad (15)$$

where $\delta m^2 = m_2^2 - m_1^2$ and θ_0 is the vacuum mixing angle. The matter potentials, V , arise from the neutrino interactions with the medium [21,22].

The above set of equations is quite complicated to solve, both because of its non-linearity and because it is momentum dependent. However, it is simplified enormously by using the so-called quantum rate equations instead of the full quantum kinetic equations presented above. In the quantum rate equations, the original quantum kinetic equations are integrated over momentum space so that the momentum dependence disappears. This integration can only be accomplished analytically if one assumes kinetic equilibrium for the neutrinos, and therefore involves an assumption. We assume that the one-particle distribution functions for neutrinos (the diagonal parts of the density matrix) are of the form $e^{-p/T}$.

The usual number densities of the mixed neutrinos are then related to the integrated density matrix by $n_\alpha = \frac{1}{2}[P_0 + P_z]$ and $n_\beta = \frac{1}{2}[P_0 - P_z]$. However, this number density is not a dimensionless quantity. In order to make \mathbf{P} and P_0 dimensionless we instead work with the dimensionless quantities $\mathbf{P}_* \equiv \mathbf{P}/n_{\nu_0}$ and $P_{0,*} \equiv P_0/n_{\nu_0}$, where n_{ν_0} is the number density of a decoupled neutrino species. As will be explained at the end of the section this also has the advantage of making the expansion of the universe simpler to treat. For simplicity we will in the remainder of the paper refrain from denoting \mathbf{P}_* and $P_{0,*}$ with an $*$.

The quantum rate equations then take the form [20]

$$\dot{\mathbf{P}} = \mathbf{V} \times \mathbf{P} - D\mathbf{P}_T - C\bar{\mathbf{P}}_T^* + [R_\alpha - R_\beta]\hat{\mathbf{z}} \quad (16)$$

$$\dot{P}_0 = R_\alpha + R_\beta \quad (17)$$

where

$$R_i = \sum_j F_{ij} [h_j n_j n_{\bar{j}} - n_{\nu_i} n_{\bar{\nu}_i}] - \frac{1}{2} \sum_l G_l \mathbf{P}_T \cdot \bar{\mathbf{P}}_T^* \quad (18)$$

$$\dot{n}_i = \sum_j F_{ij} [h_j n_j n_{\bar{j}} - n_i n_{\bar{i}}] + G_i \mathbf{P}_T \cdot \bar{\mathbf{P}}_T^*. \quad (19)$$

$h_j = 1$ for neutrinos and $h_j = \frac{1}{4}$ for electrons. The new parameters C, D, \mathbf{V}, F_{ij} and G_i are then defined as

$$C = \frac{P_0}{\bar{\mathbf{P}}_T^*} \int dp \left[\mathbf{C}(p)n(p) - \int dp' \mathbf{c}(p, p')n(p') \right] \quad (20)$$

$$D = \int dp \left[D(p)n(p) - \int dp' d(p, p')n(p') \right] \quad (21)$$

$$\mathbf{V} = \int dp \mathbf{V}(p)n(p) \quad (22)$$

$$F_{ij} = \int dp dp' dk dk' F_{ij}(pk|p'k')n(p)n(k) \quad (23)$$

$$G_i = \int dp dp' dk dk' G_i(p'k'|pk)n(p)n(k) \quad (24)$$

Some details about how to perform the phase space integrals are given in the Appendix.

In the present calculation we are interested only in a differential effect, i.e. the difference between the actual neutrino density and the density if neutrinos were completely decoupled. In that case, the quantum statistics of the involved particles is not very important [7]. In the following we therefore approximate all quantum statistics with Maxwell-Boltzmann statistics. This means that Bosons and Fermions have exactly the same behaviour.

In previous calculations of neutrino oscillations in the early universe it has been assumed that the active neutrino species have the same temperature as the electromagnetic plasma. However, that is not the case during electron-positron annihilation. We therefore have to operate with different temperatures for all the different species. Specifically we always assume a Maxwell-Boltzmann distribution with a temperature given by $T_{\text{eff},i} = T_0(n_i/n_{\nu_0})^{1/3}$, where n_{ν_0} and T_0 are the number density and temperature of a completely decoupled non-mixed neutrino species. n_i is the actual density of the given species. Electrons, positrons and photons are assumed to be in full thermal equilibrium with the temperature $T_\gamma = T_e$.

All of the above equations have been derived assuming a non-expanding universe. If the universe expands then for the usual one particle Boltzmann equation, the Liouville term df/dt is changed from $\partial f/\partial t$ to $\partial f/\partial t - Hp\partial f/\partial p$ [19]. Likewise, the left-hand side of the integrated Boltzmann equation is changed from \dot{n} to $\dot{n} + 3Hn$ [19]. However, the equations can be made to look exactly like they do for the non-expanding case if they are recast in comoving quantities. The momentum of a particle redshifts with expansion as $p \propto R^{-1}$. For the momentum dependent Boltzmann equation one then defines the comoving momentum as $p_* = pR$, a quantity that does not redshift. The Liouville operator then becomes $df/dt = \partial f/\partial t - Hp\partial f/\partial p = \partial f(p_*)/\partial t$, i.e. it looks exactly like the non-expanding case.

For the integrated Boltzmann equation this also holds. The usual procedure is to write the number densities in units of entropy density as $n_* = n/s$. If entropy is conserved n_* is not affected by cosmic expansion. However, in the present case entropy is not conserved because full thermodynamic equilibrium is not maintained. Instead one can rescale the number density in units of a completely decoupled neutrino species, $n_{\nu_0} \propto R^{-3}$. In this case the left hand side of the Boltzmann equation reads $\dot{n} + 3Hn = \dot{n}_*$. If one recasts the quantum rate equations in units of n_{ν_0} the cosmological expansion does not appear anywhere, and one can readily use Eqs. (16-24) even in an expanding universe.

A. Matter potentials

The diagonal part of the matter potential comes both from interactions with other species, and from self-interactions.

The electron lepton number is known to be small ($L_e = L_p \sim 10^{-10}$) because of charge neutrality. However the neutrino lepton numbers are not well constrained at present. At present the strongest constraints come from considering Big Bang nucleosynthesis (BBN) and Cosmic Microwave Background Radiation (CMBR) arguments. From BBN considerations one finds an upper bound on relativistic energy density (usually expressed as the effective number of neutrino species $N_\nu \equiv \rho/\rho_{\nu_0}$) [23,24], and therefore also on neutrino lepton numbers [25]. However, because electron neutrinos enter directly into the weak interactions that regulate the neutron to proton ratio an electron neutrino chemical potential cannot be directly translated into an effective number of neutrino species [25]. CMBR on the other hand is not sensitive to neutrino flavour but only to energy density. Therefore the CMBR bound on the effective number of neutrino species can be directly translated into a bound on neutrino lepton numbers [26–28]. Hansen *et al.* [29] recently combined BBN and CMBR to derive the tightest present constraint of $-0.01 < L_{\nu_e} < 0.22$ and $|L_{\nu_{\mu,\tau}}| < 2.6$ (see also [30–35]). This constraint is of course many orders of magnitude larger than the known value of the electron lepton number.

For the sake of simplicity we assume that all lepton numbers are of the same order as L_e . In that case they can be ignored in the calculation. This simplifies the numerical computations tremendously because the neutrino and anti-neutrino sectors decouple (i.e. the equations describing them are identical). However, we stress that this is not necessarily a good approximation, depending on the actual values of neutrino chemical potentials.

If one neglects all lepton numbers, the result for electron neutrinos is

$$V_e = -\frac{96\sqrt{2}G_F}{\pi^2 m_W^2} \left[T_{\nu_e} T_\gamma^4 + \frac{1}{4}(1-x)T_{\nu_e}^5 \right] \quad (25)$$

For the muon neutrino one finds a similar expression

$$V_\mu = -\frac{96\sqrt{2}G_F}{\pi^2 m_W^2} \left[\frac{1}{4}(1-x)T_{\nu_\mu}^5 \right] \quad (26)$$

This is very close to what is found using Fermi-Dirac statistics for neutrinos. For FD statistics the front factor should be $\frac{49\zeta(4)}{45\zeta(3)}\pi^2 \simeq 9.68$ [36] instead of $96/\pi^2 \simeq 9.72$ for MB. More details about the calculation of the matter potentials can be found in the Appendix.

In addition to the diagonal part of the matter potential there is an off-diagonal part due to neutrino-neutrino and neutrino-antineutrino forward scattering [37]. This term is proportional to $\int \mathbf{P}(p)dp = \mathbf{P}$, so that in the quantum rate approximation the term is identically zero. The off-diagonal term has the effect of synchronising the oscillations of different neutrino modes. However, in the quantum rate approximation the problem is reduced to following a single “effective” mode and therefore the oscillations of different modes is in some sense already synchronized. In fact there is an additional off-diagonal term which is proportional to $\rho_{\alpha\beta}$, but as will be explained in the Appendix this term is always very small.

B. Annihilation and damping terms

The annihilation term for the process $i\bar{i} \leftrightarrow j\bar{j}$ for particle i can be written as

$$R_{ij} = F_{ij} [h_j n_j n_{\bar{j}} - n_{\nu_i} n_{\bar{\nu}_i}] = \frac{4G_F^2}{\pi^3} T_{\nu_0}^5 B \left[\frac{T_j^8}{T_{\nu_0}^8} - \frac{T_i^8}{T_{\nu_0}^8} \right] \equiv F_0 B \left[\frac{T_j^8}{T_{\nu_0}^8} - \frac{T_i^8}{T_{\nu_0}^8} \right], \quad (27)$$

where B depends on the specific process. Table II lists the value of B for different processes. Again, the front factor value 4 is very close to what is found using FD statistics ($\simeq 3.97$) [36].

The same front factor can be used to calculate the damping coefficients C and D . The calculation of these terms is discussed in Ref. [20] for the case of FD statistics. Here we just state the result for MB statistics

$$D = \frac{1}{2} F_0 \left[8 \frac{T_e^4 T_{\nu_e}^4}{T_{\nu_0}^8} + 8 \frac{T_e^4 T_{\nu_\mu}^4}{T_{\nu_0}^8} + (8x^2 + 4x + 1) \frac{T_e^4 T_{\nu_e}^4}{T_{\nu_0}^8} \right] \quad (28)$$

$$+ (8x^2 - 4x + 1) \frac{T_e^4 T_{\nu_\mu}^4}{T_{\nu_0}^8} + 2 \left(\frac{T_{\nu_e}^8}{T_{\nu_0}^8} + \frac{T_{\nu_\mu}^8}{T_{\nu_0}^8} + \frac{T_{\nu_e}^4 T_{\nu_\mu}^4}{T_{\nu_0}^8} \right) \quad (29)$$

$$C = 2(16x^2 + 4) F_0 \frac{T_{\nu_e}^4 T_{\nu_\mu}^4}{T_{\nu_0}^8} \quad (30)$$

TABLE II. Values of B for different annihilation processes.

Process	B
$\nu_e \bar{\nu}_e \leftrightarrow e^+ e^-$	$8x^2 + 4x + 1$
$\nu_\mu \bar{\nu}_\mu \leftrightarrow e^+ e^-$	$8x^2 - 4x + 1$
$\nu_\tau \bar{\nu}_\tau \leftrightarrow e^+ e^-$	$8x^2 - 4x + 1$
$\nu_e \bar{\nu}_e \leftrightarrow \nu_\mu \bar{\nu}_\mu$	1
$\nu_e \bar{\nu}_e \leftrightarrow \nu_\tau \bar{\nu}_\tau$	1
$\nu_\mu \bar{\nu}_\mu \leftrightarrow \nu_\tau \bar{\nu}_\tau$	1

$$G_e = (32x^2 - 4)F_0 \frac{T_{\nu_e}^4 T_{\nu_\mu}^4}{T_{\nu_0}^8} \quad (31)$$

$$G_{\nu_\tau} = 4F_0 \frac{T_{\nu_e}^4 T_{\nu_\mu}^4}{T_{\nu_0}^8}. \quad (32)$$

These expressions are very similar to those derived by McKellar and Thomson [20] who used FD statistics but assumed identical temperatures for all species.

C. Time-temperature relationship

Fundamentally, two equations are needed to fully describe the cosmological expansion with time [2]. The system of photons and electrons/positrons can to an extremely good approximation be assumed to be in full thermal equilibrium via electromagnetic interactions, so that they can be described by a common temperature, T_γ . Therefore the two variables describing the cosmological expansion with time can be taken to be the scale factor, R , and the photon temperature, T_γ .

As the two independent equations we choose the Friedman equation [2]

$$H^2 = \frac{8\pi G\rho}{3} \quad (33)$$

and the equation of energy conservation [2]

$$d(\rho R^3) + Pd(R^3) = 0 \quad (34)$$

as our fundamental equations. These two equations can then be rewritten as equations for \dot{T}_γ and \dot{R} . Details of how to solve these equations in the case of Maxwell-Boltzmann statistics can be found in Ref. [7].

III. NUMERICAL DETAILS

We have solved the quantum rate equations, Eqs. (16-24), together with the expansion equations Eqs. (33-34), for the case of $\nu_e - \nu_\mu$ oscillations. ν_τ is in the present calculation assumed to be non-mixed. As initial conditions we choose $T_\nu = T_\gamma = 15$ MeV, a temperature well above the electron-positron annihilation temperature $T_{\text{ann}} \sim 0.3$ MeV. Furthermore we set $P_x = P_y = P_z = 0$ and $P_0 = 2$ (and identically for anti neutrinos). However, the outcome is not sensitive to initial conditions in the mixed neutrino sector because at high temperatures \mathbf{P} is quickly driven to zero because of fast interactions, no matter what its initial value is. The system of equation is then straightforward to solve.

Fig. 1 shows the evolution of n_{ν_e} , n_{ν_μ} , and n_{ν_τ} for different values of the mixing angle, calculated for the specific value of the mass difference $\delta m^2 = 3 \times 10^{-5} \text{ eV}^2$. This figure also shows the limiting case of non-mixed neutrinos ($\sin 2\theta_0 = 0$).

It should be noted that the result of the non-mixed case is quite close to the result found by elaborate momentum-dependent calculations. The calculation by Dodelson and Turner [7] used the same approximation as we have in the present work (i.e. zero electron mass and Boltzmann statistics for all particles), except that they solved the full momentum dependent Boltzmann equation for the non-mixed case. Their result was approximately $\delta\rho_{\nu_e}/\rho_{\nu_0} \simeq 0.012$

and $\delta\rho_{\nu_\mu}/\rho_{\nu_0} \simeq 0.005$, whereas our result for the non-mixed case is $\delta\rho_{\nu_e}/\rho_{\nu_0} \simeq 0.0124$ and $\delta\rho_{\nu_\mu}/\rho_{\nu_0} \simeq 0.0057$. This shows that although our calculation is quite crude in the sense that it does not fully account for momentum dependence it yields results which are fairly close to momentum dependent calculations, at least for the case of non-mixed neutrinos. We do expect the same to be true for the mixed case, although this remains to be verified.

Calculations which have used exact quantum statistics and electron mass give slightly smaller neutrino heating. Hannestad and Madsen found 0.0083 for ν_e and 0.0041 for ν_μ [9], whereas Dolgov, Hansen and Semikoz found 0.009 and 0.004 [10,11]. The most recent treatment by Gnedin and Gnedin found 0.0097 and 0.0062 [12].

In Fig. 2 we show the evolution of $P_z = n_{\nu_e} - n_{\nu_\mu}$ for different values of the mixing angle. It is clear that for this specific choice of δm^2 a very large mixing angle is needed to achieve a noticeable effect. $\delta m^2 = 3 \times 10^{-5} \text{ eV}^2$ is of the same order of magnitude as the best fitting solutions for the LMA ($\delta m^2 = 4.5 \times 10^{-5} \text{ eV}^2$) and SMA ($\delta m^2 = 4.7 \times 10^{-6} \text{ eV}^2$) solutions to the solar neutrino problem. Therefore it is clear that for the SMA solution where the best fit at present is $\sin 2\theta_0 \simeq 0.04$ there will be no noticeable effect of neutrino oscillations on neutrino heating. On the other hand for the LMA solution $\sin 2\theta_0 \simeq 0.91$ which is large to enough to give a significant change.

The evolution of P_z with temperature can be understood as follows. At high temperatures oscillations are suppressed by the matter potential, and therefore P_z evolves independently of the mixing angle. However at a certain temperature the matter mixing angle goes through a maximum and oscillations become an important equilibration factor. The rate of equilibration between the two species is to a rough approximation given by $\Gamma_{\text{eq}} \sim D \cos^2 2\theta \sin^2 2\theta$ [38]. This should be compared with the rate at which the abundances are driven apart by interactions with the electron-positron plasma, $\Gamma_{\text{drive}} \sim (R_e - R_\mu)$. The matter mixing angle is given by the expression

$$\sin^2 2\theta = \sin^2 2\theta_0 / (1 - 2f \cos 2\theta_0 + f^2), \quad (35)$$

where $f \equiv 6T(V_e - V_\mu)/\delta m^2$. This mixing angle goes through a maximum when $f = \cos 2\theta_0$ which also corresponds to a maximum in the equilibration rate. This maximum occurs exactly at the temperature where the dip in P_z is seen. Below this temperature the mixing angle approaches the vacuum value and $\Gamma_{\text{eq}}/\Gamma_{\text{drive}}$ approaches a constant value, which to a reasonable approximation is

$$\frac{\Gamma_{\text{eq}}}{\Gamma_{\text{drive}}} \rightarrow \frac{8}{16x^2 + 2} \left(\frac{4}{11} \right)^{4/3} \sin^2 2\theta_0 \cos^2 2\theta_0. \quad (36)$$

This asymptotic value is always smaller than one so that for small temperatures P_z follows the same trend independently of the vacuum mixing angle because the driving term is dominant. However, as the vacuum mixing angle increases the equilibration around the maximum of the mixing angle becomes more and more important. Therefore the final value of P_z decreases strongly with increasing vacuum mixing angle.

Oscillations in general become important once the matter potential no longer dominates the vacuum oscillation term. This happens when

$$T_{\text{MeV}} < \left(\frac{\delta m^2 \cos 2\theta_0}{1.0 \times 10^{-7} \text{ eV}^2} \right)^{1/6} \quad (37)$$

For the large value of δm^2 in Fig. 2 this temperature is above the decoupling temperature for neutrinos. Therefore once the oscillations become important they are quickly damped and no oscillation pattern is seen at lower temperatures.

This is not the case for lower values of δm^2 where oscillations only become important well after neutrino decoupling. In Fig. 3 we show the evolution of P_z for various values of δm^2 . For $\delta m^2 = 10^{-6} \text{ eV}^2$ the oscillations are completely damped away because neutrinos have not decoupled before oscillations become important. For $\delta m^2 = 10^{-8} \text{ eV}^2$ oscillations are apparent, but still of very low amplitude. Notice that at low temperatures the mean of the oscillating curve still rises slowly due to neutrino heating by the electron-positron annihilations. Finally, for $\delta m^2 = 10^{-10} \text{ eV}^2$ neutrinos have decoupled completely before oscillations become important. This means that there is effectively no damping of neutrino oscillations once they commence.

Therefore, for low values of δm^2 , P_z does not approach a definite value for low temperatures, even though the total neutrino number density, P_0 , does.

Of course the oscillation of P_z at low temperature is an artifact of the quantum rate approximation. In the momentum dependent treatment different modes oscillate with different frequencies and oscillations decohere because of this effect. However, it should be noted that if neutrino lepton numbers are significant, this picture can change completely [39]. In that case the off-diagonal elements in the neutrino matter potential are large, and neutrino oscillations become coherent. As long as all lepton numbers can be neglected, as was assumed in the present treatment,

it will make better sense to use the average of P_z instead of the actual value because the decoherence effect was not accounted for.

The increase in oscillation amplitude seen for decreasing δm^2 is also seen for active-sterile oscillations, for the same reason [36].

One non-standard feature in the active-active oscillations is the appearance of the interference terms in the Boltzmann equation. These terms could potentially be important and lead to a different result for neutrino heating. However, it turns out that they are always completely negligible compared with the usual collision terms. Fig. 3 shows the quantity $Q \equiv \frac{1}{2} \sum_i G_i \mathbf{P}_T \cdot \bar{\mathbf{P}}_T^* / \sum_j F_{ij} [h_j n_j n_{\bar{j}} - n_{\nu_i} n_{\bar{\nu}_i}]$ for $i = \nu_e$, for the specific case of $\delta m^2 = 3 \times 10^{-5} \text{ eV}^2$, $\sin 2\theta_0 = 0.5$. This clearly shows that the non-standard terms from annihilation of mixed states is tiny compared with the standard Boltzmann terms and that they can be safely ignored in numerical treatments.

IV. DISCUSSION

We have solved the Boltzmann equations governing the evolution of neutrinos around the time of their decoupling from equilibrium, including effects due to mixing of ν_e and ν_μ . We always assumed that the tau neutrino is unmixed.

As could be expected oscillations have the effect of bringing the ν_e and ν_μ abundances closer together. Strong oscillations also have an effect on the total neutrino energy density after electron-positron annihilation. The reason is that without oscillations, most of the heating is to the ν_e sector because electron neutrinos have charged current interactions. Oscillations drain away electron neutrinos into muon neutrinos, and therefore the back-reaction $\nu_e \bar{\nu}_e \rightarrow e^+ e^-$ decreases in efficiency. The end result is a slightly larger neutrino energy density. As is customary we parametrise the neutrino energy density in units of the energy density of a decoupled massless neutrino, $N_\nu = \rho_\nu / \rho_{\nu_0}$ (so that in the absence of neutrino heating $N_\nu = 3$). However, it is also necessary to account for the slightly lower photon temperature if neutrino heating is accounted for, because all quantities should be measured relative to the actual photon temperature. We therefore use the definition

$$N_\nu = \frac{\rho_\nu}{\rho_{\nu_0}} \frac{\rho_{\gamma_0}}{\rho_\gamma} \quad (38)$$

In Fig. 5 we plot the N_ν at low temperature. From this figure it can be seen that neutrino oscillations can change the effective number of neutrino species by about 6×10^{-4} . The effective number of neutrino species without oscillations is $N_\nu = 3.0467$, and in the limit of large mass difference and mixing angle it approaches $N_\nu = 3.0479$. This value is somewhat higher than what is found in the more thorough calculations using FD statistics and the full momentum dependent Boltzmann equation ($N_\nu = 3.028$ [9], $N_\nu = 3.034$ [10,11], $N_\nu = 3.032$ [12]) simply because of the larger neutrino heating when MB statistics is used (our value fits very well with that of Ref. [7], who found $N_\nu = 3.046$ using MB statistics).

For BBN calculations, there is an additional effect which must be considered. The electron neutrinos have a different effect on BBN than muon or tau neutrinos because they enter directly in the β -reaction which regulate the neutron to proton ratio. An increased number of electron neutrinos and anti-neutrinos have the effect of increasing the $n - p$ conversion efficiency. This in turn leads to a lower neutron to proton ratio at helium formation and in turn a lower helium abundance. This effect works in the opposite direction of a simple increase in N_ν . Furthermore, because of energy conservation the photon temperature is slightly lower if neutrino heating is included because photon heating by $e^+ e^-$ annihilation is slightly smaller. This also has the effect of lowering the $n - p$ conversion rate because there are slightly fewer electrons and positrons.

To get a feeling for how neutrino oscillations change the helium production we have modified the Kawano nucleosynthesis code [40] to take into account neutrino heating. We have then performed the numerical calculation for oscillation parameters corresponding to the best fit for the LMA solar neutrino solution ($\sin 2\theta_0 = 0.908$ and $\delta m^2 / \text{eV}^2 = 4.5 \times 10^{-5}$). The result is shown in Table III, together with our result for the case of no oscillations and the limiting case of large δm^2 and $\sin 2\theta_0$.

This shows that more helium is produced for the oscillating case. The main reason for this is the lower density of electron neutrinos in the case of mixing, but the increase in the effective number of neutrino species also leads to an increase in helium production. Interestingly, the change in helium abundance due to oscillations is of the same order of magnitude as the total effect. The reason is that in the non-oscillating case the effect on helium is very small because of cancellations. The increase in electron neutrino temperature is roughly compensated by the increase in the effective number of neutrinos, as well as the decrease in photon temperature. Oscillations destroy this accidental cancellation and therefore have a large effect. Our finding for the non-oscillating case fits well with other calculations.

TABLE III. Change in helium abundance due to neutrino heating, for the case of $\eta_{10} = 5 \times 10^{-10}$.

Solution	$\delta m^2 / \text{eV}^2$	$\sin 2\theta_0$	$\delta \rho_{\nu_e} / \rho_{\nu_0}$	$\delta \rho_{\nu_\mu} / \rho_{\nu_0}$	$\delta \rho_{\nu_\tau} / \rho_{\nu_0}$	ΔY_P
LMA	4.5×10^{-5}	0.908	0.0097	0.0087	0.0057	2.0×10^{-4}
No osc.	-	-	0.0124	0.0057	0.0057	1.2×10^{-4}
Maximal mixing	-	-	0.0093	0.0093	0.0058	2.2×10^{-4}

 TABLE IV. Change in helium abundance due to neutrino heating, for the case of $\eta_{10} = 5 \times 10^{-10}$. Results are from assuming infinitely tight coupling between ν_μ and ν_τ .

Solution	$\delta m^2 / \text{eV}^2$	$\sin 2\theta_0$	$\delta \rho_{\nu_e} / \rho_{\nu_0}$	$\delta \rho_{\nu_\mu} / \rho_{\nu_0}$	$\delta \rho_{\nu_\tau} / \rho_{\nu_0}$	ΔY_P
LMA	4.5×10^{-5}	0.908	0.0089	0.0077	0.0077	2.3×10^{-4}
No osc.	-	-	0.0124	0.0057	0.0057	1.2×10^{-4}
Maximal mixing	-	-	0.0082	0.0082	0.0082	2.5×10^{-4}

Using the same approximations as in the present paper Fields, Dodelson and Turner [8] found $\Delta Y_P = 1.1 \times 10^{-4}$. More sophisticated methods find similar values in the range $\Delta Y_P = 1.1 - 1.5 \times 10^{-4}$.

In terms of energy density the changes to neutrino heating by neutrino oscillations are quite small. If indeed the large mixing angle solution turns out to be correct then the effective number of neutrino species is changed by roughly 4×10^{-4} compared to the non-oscillating case. From CMBR the present bound on the effective number of neutrino species is $N_\nu < 13$ [27,28], i.e. more than two orders of magnitude larger than the effect induced by neutrino heating, and about 10^4 times bigger than the change induced by oscillations. With precision data from upcoming satellite experiments such as the Planck Surveyor it could be possible to measure $\Delta N_\nu \simeq 0.04$ [41] which is comparable to the effect from neutrino heating. Even so the small difference induced by oscillations will likely remain undetectable.

For BBN the change due to neutrino heating is of the order 10^{-4} . At present the observational uncertainty on the primordial helium abundance is about $\sigma(Y_P) \sim 0.005$ [24], which is about 50 times larger than the change. Here, however, the change due to neutrino heating is more significant, comparable in magnitude to the total neutrino heating effect. It is perhaps conceivable that the difference in neutrino heating from including oscillations could be detected.

Finally, we stress that the present treatment is by no means definitive. A proper treatment of momentum dependence is missing, as is the inclusion of three-neutrino oscillations. Inclusion of momentum dependence is not likely to have a big effect for the relatively large mass difference and mixing angle characterising the LMA solution, but may be important for the vacuum solution. If ν_μ and ν_τ are maximally mixed, as is indicated by atmospheric neutrino measurements, then they will behave effectively as one species during neutrino decoupling. This should have the effect of lowering the electron neutrino temperature more than for two-neutrino oscillations, while increasing the overall effective number of neutrino species slightly. Altogether this amounts to the same effect as for two-neutrino oscillations, but slightly larger.

It is simple to calculate the extreme upper limit on the oscillation effect by considering a complete coupling of ν_μ and ν_τ . In Table IV we show results of the same calculation as in Table III, but now assuming an infinitely tight coupling between muon and tau neutrinos. This is likely to be a very good approximation to the true state of affairs, because the preferred values of the mixing parameters for $\nu_\mu - \nu_\tau$ mixing is at present [18] ($\delta m^2 \simeq 2 \times 10^{-3} \text{eV}^2$, $\sin 2\theta_0 \simeq 1$). This means that oscillations become important already when $T \simeq 5 \text{MeV}$, long before neutrinos decouple and also long before neutrino heating commences. Therefore in this case, ν_μ and ν_τ should be treated as having effectively the same temperature. Note that this is only a good approximation when θ_{13} is small so that there is little direct mixing of ν_e and ν_τ . Observations indeed indicate that this is the case.

Maximal coupling between the muon and tau neutrinos therefore lead to a slightly larger increase in energy density due to neutrino heating. In the case of maximal $\nu_e - \nu_\mu$ coupling it increase N_ν from 3.0479 to 3.0484, and for the LMA solution from 3.0476 to 3.0478. Helium production is also slightly increased, by about 0.2×10^{-4} . Although we have not performed a full three-neutrino oscillation calculation, this estimate should be fairly close to the true value because ν_μ and ν_τ are most likely maximally mixed with a large mass difference [18].

ACKNOWLEDGMENTS

I wish to thank Dmitri Semikoz, Sergio Pastor, and Georg Raffelt for valuable comments.

V. APPENDIX

A. Matter potentials

The diagonal matter potentials arise from neutrino loop interactions with the background medium. The magnitude of the potentials were first calculated by Nötzold and Raffelt [21] (see also [22]). In the absence of lepton numbers, there is no contribution due to interactions with neutrinos of different flavour. Neutrinos of the same flavour yield the contribution

$$V = \frac{16\sqrt{2}G_F p}{3m_Z^2} \langle E_\nu \rangle N_\nu. \quad (39)$$

For electron neutrinos there is an additional contribution from interactions with the background electrons and positrons. If the electron mass is neglected the contribution is

$$V = \frac{16\sqrt{2}G_F p}{3m_W^2} \langle E_e \rangle N_e. \quad (40)$$

Neglecting the electron mass in the matter potentials only leads to very small errors and is consistent with neglecting it in the interaction matrix elements. In the quantum rate approximation one should make the replacement $p \rightarrow \langle E_\nu \rangle = 3T_\nu$. Then using $N_e = 2T_\gamma^3/\pi^2$ and $N_\nu = T_\nu^3/\pi^2$, one finds

$$V_e = -\frac{96\sqrt{2}G_F}{3\pi^2 m_W^2} \left[T_{\nu_e} T_\gamma^4 + \frac{1}{4}(1-x)T_{\nu_e}^5 \right] \quad (41)$$

for the electron neutrinos. For the muon neutrino there is no contribution from electrons, and one finds the result

$$V_\mu = -\frac{96\sqrt{2}G_F}{3\pi^2 m_W^2} \left[\frac{1}{4}(1-x)T_{\nu_\mu}^5 \right] \quad (42)$$

As was mentioned in Section II.a there is an additional off-diagonal term which is of the form [20]

$$V = \frac{8\sqrt{2}G_F p}{3m_Z^2} \langle E_\nu \rangle \rho_{\alpha\beta}. \quad (43)$$

However, because the off-diagonal elements of $\rho_{\alpha\beta}$ are always very small until long after neutrino freeze-out this contribution is negligible.

B. Phase-space integrals

In this section we discuss how to perform the phase-space integrals needed to calculate the terms in Eqs. (32). A full derivation of all the terms would be too lengthy, but as a representative example we show the calculation of the contribution to R_e by the process $\nu_e \bar{\nu}_e \leftrightarrow e^+ e^-$.

$$R_e(\nu_e \bar{\nu}_e \leftrightarrow e^+ e^-) = \frac{1}{n_{\nu_e}} \int dp dp' dk dk' (2\pi)^4 V^2 (pk|p'k') \delta(p+k-p'-k') [f_e(p')f_e(k') - f_{\nu_e}(p)f_{\nu_e}(k)] \quad (44)$$

Here, $dp \equiv \frac{d^3 p}{2p_0(2\pi)^3}$, $f_e(p') = e^{-p'/T_e}$, and $f_{\nu_e}(p) = e^{-p/T_{\nu_e}}$. All quantities are normalized to the density of a single decoupled neutrino species, which explains the $\frac{1}{n_{\nu_e}}$ in front.

The squared matrix element is

$$V^2(pk|p'k') = 32G_F^2[(2x+1)^2(p \cdot k')(k \cdot p') + (2x)^2(p \cdot p')(k \cdot k')]. \quad (45)$$

Because of the Boltzmann statistics, $f_e(p')f_e(k') = f_e(p)f_e(k)$. Using this, the dp', dk' integrals can be performed using Lenard's formula

$$\int \frac{d^3p'}{2p'_0} \frac{d^3k'}{2k'_0} \delta(P - p' - k') p'^\mu k'^\nu = \frac{\pi}{24} (2P^\mu P^\nu + g^{\mu\nu} P^2) \quad (46)$$

The result is

$$R_e(\nu_e \bar{\nu}_e \leftrightarrow e^+ e^-) = \frac{1}{n_{\nu_0}} \frac{16}{3} \frac{\pi G_F^2}{(2\pi)^8} (8x^2 + 4x + 1) \times \int \frac{d^3p}{2p_0} \frac{d^3k}{2k_0} [e^{-p/T_e} e^{-k/T_e} - e^{-p/T_{\nu_e}} e^{-k/T_{\nu_e}}] (p \cdot k)^2 \quad (47)$$

We then use that $(p \cdot k)^2 = p^2 k^2 (1 - \cos \theta)^2$, where θ is the angle between the direction of p and k . After performing the integrals over d^3p and d^3k the result is then

$$R_e(\nu_e \bar{\nu}_e \leftrightarrow e^+ e^-) = \frac{1}{n_{\nu_0}} \frac{4G_F^2}{\pi^5} (8x^2 + 4x + 1) [T_e^8 - T_{\nu_e}^8] \quad (48)$$

Using $n_{\nu_0} = T_{\nu_0}^3/\pi^2$ the contribution to the Boltzmann collision integral is

$$R_e(\nu_e \bar{\nu}_e \leftrightarrow e^+ e^-) = \frac{4G_F^2}{\pi^3} T_{\nu_0}^5 (8x^2 + 4x + 1) \left[\frac{T_e^8}{T_{\nu_0}^8} - \frac{T_{\nu_e}^8}{T_{\nu_0}^8} \right] \quad (49)$$

This result is almost identical to what is found using FD statistics (3.97 in the front factor instead of 4).

- [1] See for instance L. Bergström and A. Goobar, "Cosmology and particle astrophysics," *Chichester, UK: Wiley (1999) 344 p.*
- [2] See for instance E. W. Kolb and M. S. Turner, "The Early Universe," *Redwood City, USA: Addison-Wesley (1990) 547 p. (Frontiers in physics, 69).*
- [3] D. A. Dicus, E. W. Kolb, A. M. Gleeson, E. C. Sudarshan, V. L. Teplitz and M. S. Turner, *Phys. Rev. D* **26**, 2694 (1982).
- [4] N. C. Rana and B. Mitra, *Phys. Rev. D* **44**, 393 (1991).
- [5] M. A. Herrera and S. Hacyan, *Astrophys. J.* **336**, 539 (1989).
- [6] A. D. Dolgov and M. Fukugita, *Phys. Rev. D* **46**, 5378 (1992).
- [7] S. Dodelson and M. S. Turner, *Phys. Rev. D* **46**, 3372 (1992).
- [8] B. D. Fields, S. Dodelson and M. S. Turner, *Phys. Rev. D* **47**, 4309 (1993) [arXiv:astro-ph/9210007].
- [9] S. Hannestad and J. Madsen, *Phys. Rev. D* **52**, 1764 (1995) [arXiv:astro-ph/9506015].
- [10] A. D. Dolgov, S. H. Hansen and D. V. Semikoz, *Nucl. Phys. B* **503**, 426 (1997) [arXiv:hep-ph/9703315].
- [11] A. D. Dolgov, S. H. Hansen and D. V. Semikoz, *Nucl. Phys. B* **543**, 269 (1999) [arXiv:hep-ph/9805467].
- [12] N. Y. Gnedin and O. Y. Gnedin, *Astrophys. J.* **509**, 11 (1998).
- [13] S. Esposito, G. Miele, S. Pastor, M. Peloso and O. Pisanti, *Nucl. Phys. B* **590**, 539 (2000) [arXiv:astro-ph/0005573].
- [14] G. Steigman, arXiv:astro-ph/0108148.
- [15] P. Langacker, S. T. Petcov, G. Steigman and S. Toshev, *Nucl. Phys. B* **282**, 589 (1987).
- [16] See the URL http://www.sno.phy.queensu.ca/sno/first_results/
- [17] J. N. Bahcall, M. C. Gonzalez-Garcia and C. Pena-Garay, *JHEP* **0108**, 014 (2001) [arXiv:hep-ph/0106258].
- [18] Y. Fukuda *et al.* [Super-Kamiokande Collaboration], *Phys. Rev. Lett.* **81**, 1562 (1998) [arXiv:hep-ex/9807003].
- [19] J. Bernstein, "Kinetic Theory In The Expanding Universe," *CAMBRIDGE, USA: UNIV. PR. (1988) 149p.*
- [20] B. H. McKellar and M. J. Thomson, *Phys. Rev. D* **49**, 2710 (1994).
- [21] D. Nötzold and G. Raffelt, *Nucl. Phys. B* **307**, 924 (1988).
- [22] K. Enqvist, K. Kainulainen and J. Maalampi, *Nucl. Phys. B* **349**, 754 (1991).
- [23] E. Lisi, S. Sarkar and F. L. Villante, *Phys. Rev. D* **59**, 123520 (1999) [arXiv:hep-ph/9901404].
- [24] K. A. Olive, G. Steigman and T. P. Walker, *Phys. Rept.* **333**, 389 (2000) [arXiv:astro-ph/9905320].
- [25] H. S. Kang and G. Steigman, *Nucl. Phys. B* **372**, 494 (1992).

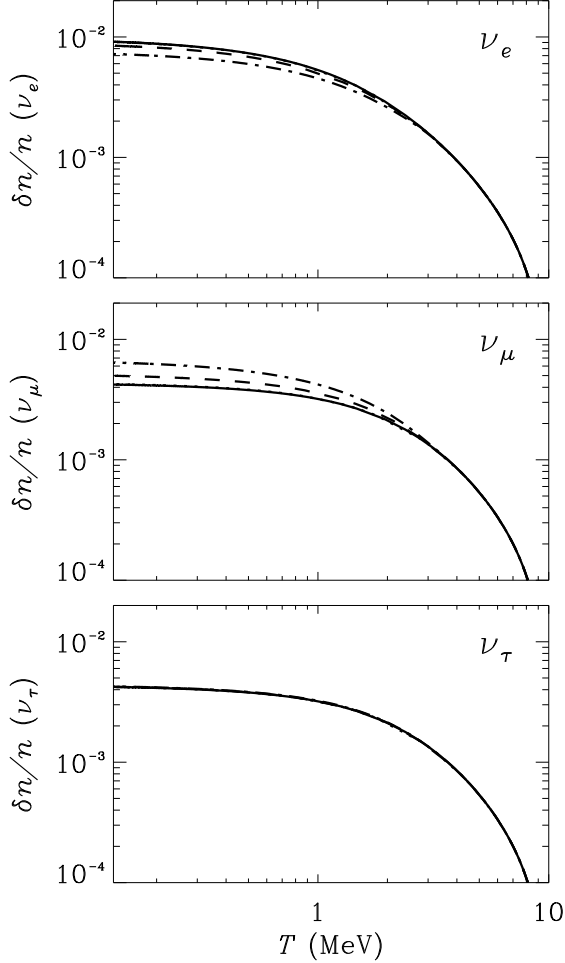


FIG. 1. The evolution of $\delta n/n$ for electron, muon and tau neutrino for $\delta m^2 = 3 \times 10^{-5} \text{eV}^2$, plotted for different values of the vacuum mixing angle. The full line is for $\sin 2\theta_0 = 0$, the dotted for $\sin 2\theta_0 = 0.1$, the dashed for $\sin 2\theta_0 = 0.5$ and the dot-dashed for $\sin 2\theta_0 = 0.9$.

- [26] J. Lesgourgues and S. Pastor, Phys. Rev. D **60**, 103521 (1999) [arXiv:hep-ph/9904411].
- [27] S. Hannestad, Phys. Rev. Lett. **85**, 4203 (2000) [arXiv:astro-ph/0005018].
- [28] S. Hannestad, Phys. Rev. D **64**, 083002 (2001) [arXiv:astro-ph/0105220].
- [29] S. H. Hansen, G. Mangano, A. Melchiorri, G. Miele and O. Pisanti, arXiv:astro-ph/0105385.
- [30] S. Esposito, G. Mangano, G. Miele and O. Pisanti, JHEP **0009**, 038 (2000) [arXiv:astro-ph/0005571].
- [31] M. Orito, T. Kajino, G. J. Mathews and R. N. Boyd, arXiv:astro-ph/0005446.
- [32] S. Esposito, G. Mangano, A. Melchiorri, G. Miele and O. Pisanti, Phys. Rev. D **63**, 043004 (2001) [arXiv:astro-ph/0007419].
- [33] J. P. Kneller, R. J. Scherrer, G. Steigman and T. P. Walker, arXiv:astro-ph/0101386.
- [34] A. R. Zentner and T. P. Walker, arXiv:astro-ph/0110533.
- [35] R. H. Cyburt, B. D. Fields and K. A. Olive, arXiv:astro-ph/0105397.
- [36] K. Enqvist, K. Kainulainen and M. J. Thomson, Nucl. Phys. B **373**, 498 (1992).
- [37] J. Pantaleone, Phys. Lett. B **287**, 128 (1992).
- [38] G. G. Raffelt, "The astrophysics of neutrinos, axions, and other weakly interacting particles," *Chicago, USA: Univ. Pr. (1996) 664 p.*
- [39] S. Pastor, G. G. Raffelt and D. V. Semikoz, arXiv:hep-ph/0109035.
- [40] L. Kawano, FERMILAB-PUB-92-04-A.
- [41] R. E. Lopez, S. Dodelson, A. Heckler and M. S. Turner, Phys. Rev. Lett. **82**, 3952 (1999) [arXiv:astro-ph/9803095].

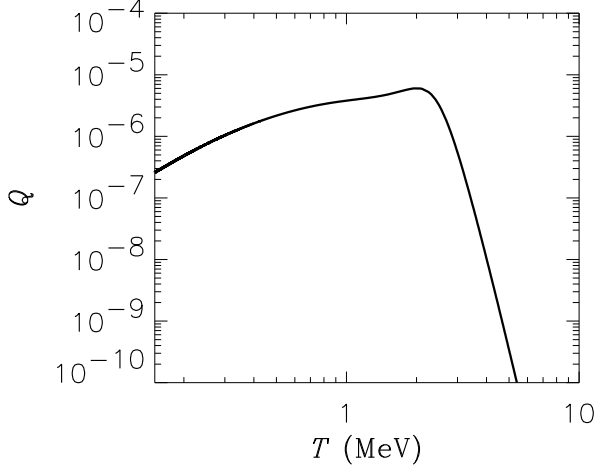


FIG. 2. The evolution of the parameter $Q \equiv \frac{1}{2} \sum_i G_i \mathbf{P}_T \cdot \bar{\mathbf{P}}_T^* / \sum_j F_{ij} [h_j n_j n_{\bar{j}} - n_{\nu_i} n_{\bar{\nu}_i}]$ for $i = \nu_e$, for the specific case of $\delta m^2 = 3 \times 10^{-5} \text{ eV}^2$, $\sin 2\theta_0 = 0.5$.

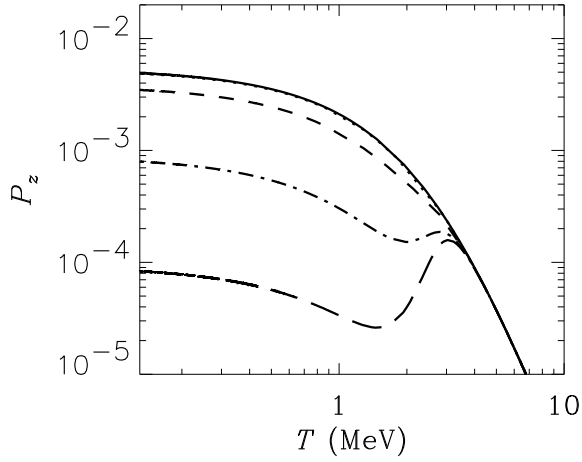


FIG. 3. The temperature evolution of $P_z \equiv n_{\nu_e} - n_{\nu_\mu}$ for $\delta m^2 = 1.0 \times 10^{-5} \text{ eV}^2$ for various different values of $\sin 2\theta_0 = 0$. The full line is for $\sin 2\theta_0 = 0$, the dotted for $\sin 2\theta_0 = 0.1$, the dashed for $\sin 2\theta_0 = 0.5$, the dot-dashed for $\sin 2\theta_0 = 0.9$, and the long-dashed for $\sin 2\theta_0 = 0.99$.

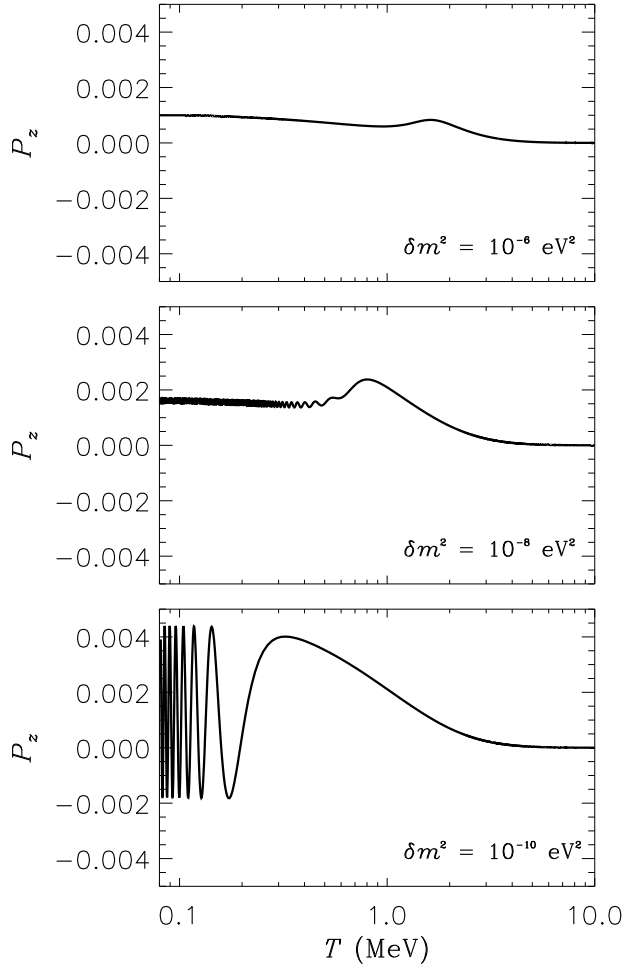


FIG. 4. The temperature evolution of $P_z \equiv n_{\nu_e} - n_{\nu_\mu}$ for $\sin 2\theta_0 = 0.9$ for various different values of δm^2 . The upper panel is for $\delta m^2 = 1.0 \times 10^{-6} \text{eV}^2$, the middle for $\delta m^2 = 1.0 \times 10^{-8} \text{eV}^2$ and the lower for $\delta m^2 = 1.0 \times 10^{-10} \text{eV}^2$.

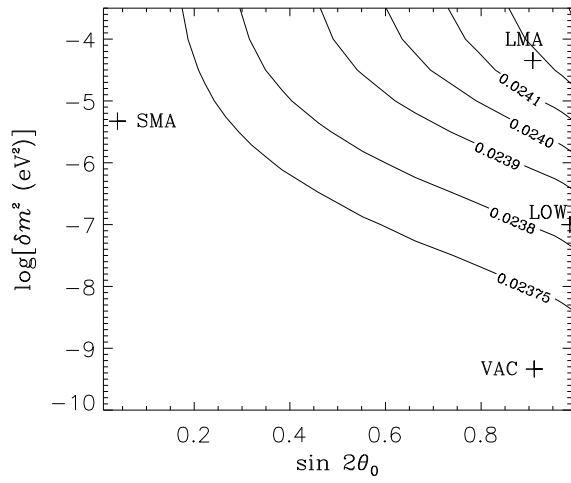


FIG. 5. The total change in effective number of neutrino species ($\Delta N_\nu = N_\nu - 3$) as a function of δm^2 and $\sin 2\theta_0$. Shown are also the best fit values for the possible solar neutrino solutions [17].